BULLETIN OF THE POLISH ACADEMY OF SCIENCES
TECHNICAL SCIENCES, Vol. 70(2), 2022, Article number: e140373
DOI: 10.24425/bpasts.2022.140373

Multi-criteria diagnostics of historic buildings with the use of 3D laser scanning (a case study)

Anna SZYMCZAK-GRACZYK[1]*, Zbigniew WALCZAK[1], Barbara KSIT[2], and Zdzisław SZYGUŁA[3]

[1] Department of Construction and Geoengineering, Poznan University of Life Sciences, 60-637 Poznań, Poland
[2] Institute of Building Engineering, Poznan University of Technology, Piotrowo 5, 60-965 Poznań, Poland
[3] Company owner, Poland

Abstract. The protection and use of historic buildings is a difficult and costly task. Most often, these objects are under conservatory protection and any interference in their structure requires appropriate consent. On the other hand, conducting construction works on historic buildings carries a high risk of their damage or even destruction. Therefore, proper prior diagnostics is an extremely important factor affecting the scope and manner of works to be conducted. The paper presents the use of 3D scanning to determine the deflection of the ceiling under the Column Hall of the historic Palace, the floor of which showed elasticity, recorded during changing service loads. After identifying the places with the greatest deflections, based on data from 3D laser scanning, test holes were made and wood samples from the ceiling were taken to perform moisture content and mycological tests. An endoscopic inspection camera was inserted into test holes, providing the basis for recognizing the structure of the ceiling, i.e. arrangement of layers as well as dimensions and spacing of ceiling beams. Strength calculations were made with the limit state method resulted in the determination of the maximum permissible service load on the ceiling. The presented course of action in diagnostics of the analysed historic building may be an example of a preliminary procedure to be taken before deciding on changes in the manner of use of historic buildings or the functionalities of their individual parts.

Key words: laser scanning; diagnostics; historic buildings; limit state method; beam deflection; mycological tests.

1. INTRODUCTION

"We are responsible for the world's heritage, but it will take the form we give it." The words by André Malraux provide elemental advice for the protection of cultural and historic heritage. It is a difficult and multi-threaded process in which the role limited to being a guardian of a monument might not be considered sufficient. Nowadays, historic buildings are being rediscovered, and they are performing more and more commercial and service functions. However, for historic buildings to fulfil these extended functionalities, ongoing diagnostics should be carried out to verify the safety of their use from the structural point, but primarily, from the perspective of people who stay in them and use them. Diagnostics of historic buildings is a complicated issue as it is not easy to carry out acceptable repairs and feasible reinforcements in such facilities. Most often, it is also impossible to perform a full range of destructive tests to check the technical condition of buildings due to historic matter loss. On the other hand, failure to renovate historic buildings leads to their degradation and destruction [1–3].

One of the non-invasive techniques used to obtain information about the geometry of objects is 3D laser scanning. Terrestrial Laser Scanning (TLS) [4] is a technology widely used in reverse engineering to quickly obtain detailed 3D information (x, y, z point coordinates) in the form of a cloud of points in space. 3D laser scanning is currently used, among others, in inventory [5–9], supervision [10, 11], verification of test results [12], and conservation of building objects, primarily with historic and cultural heritage significance [13]. Undoubtedly, TLS is one of the quick methods of obtaining information on the geometry of objects. For instance, inventory can be carried out faster and more accurately than using traditional solutions. The accuracy of the created model may vary from a few millimetres [14, 15] to even decimetres [16]. It may depend, inter alia, on the distance and angle between the scanner and the scanned object, as well as on the type of scanned surfaces, as it particularly occurs with highly reflective, mirror-like surfaces [17–19]. Another advantage is that TLS allows us to obtain full, three-dimensional information on objects in the form of a point cloud that can be then processed. Therefore, it seems to be a good alternative to traditional methods. A few inconveniences, however, should be noted, such as some scanned elements may be invisible or inaccessible for the scanning laser; glass elements (windows, mirrors), but also damp ones, with water, may cause interference. Additionally, a large resultant data set may cause problems in further processing due to significant hardware requirements.

Problems related to the lack of laser access to the areas that are scanned may be solved by the use of the technique that combines laser measurements with manual measurements [20] and photogram- metry [2, 21, 23–26]. Fawzy [23] indicates that the combination of TLS techniques and short-range photogrammetry increases the accuracy of the model supporting it with the analyses carried out for the mosque of Kafrelsheikh University campus based on measurements of 20 points, 10 lines,

*e-mail: anna.szymczak-graczyk@up.poznan.pl

Manuscript submitted 2021-07-13, revised 2021-10-04, initially accepted for publication 2021-11-25, published in April 2022.

and 6 control angles. The measurements were made using the SOKKIA CX-105 total station, considering the obtained results as referential, supplementing them with photogrammetric survey and laser scanner techniques. The authors point out that the maximum improvement in model quality was 80.1, 66.4, and 84.2% for points, lines, and angles, respectively.

More and more often, for renovation and revitalisation of historic buildings, the Heritage or Historic Building Information Modelling (HBIM) technology is being used, which enables to build a 3D model of an object and use it when planning modernisation, revitalisation, operation, or even visualisation of the facility [22, 27–32]. The use of TLS can also help assess the technical condition of the building since it can significantly facilitate damage assessment and appropriate systematic renovation propositions [11]. The accuracy of point clouds is sufficient to perform surface regularity checks.

Fungi can play a significant role in the degeneration of cultural heritage and museum objects, primarily those susceptible to their effects [33, 34]. They can also adversely affect people staying longer in rooms, facilities where the process of mycelium development is intensified [35]. One of the key reasons why fungi are a great problem in cultural heritage protection is the lack of information and training for conservators, curators, and other museum personnel [36]. The occurrence of fungi is, therefore, a consequential element in the assessment of the technical condition of objects, specifically historic ones. However, non-destructive methods are not always able to show the presence of mycelium in structures, particularly when the analysis must be carried out on elements that are difficult to access or to which no direct access is available.

The paper shows the course of action when determining the bearing and strength capacity of a ceiling in a particular historic building using non-destructive research methods. Laser scanning was used to estimate changes in the ceiling geometry. This facilitated selecting the places for test holes made to examine the structure of the ceiling with an endoscopic camera and performing moisture content and mycological tests. The work is a case study, which consisted in verifying whether this historic building and precisely, its truly representative Column Hall, could fulfil a commercial function. Since the scope of destructive tests in the building was highly limited due to being under the protection of the conservator-restorer, it was even more important to thoroughly determine the places for test holes to minimize damage to the matter of the object. Although the functional extension of historic buildings always leads to changes in acting service loads, these increases cannot result in a risk of a construction failure or catastrophe [37]. The paper presents the results of diagnostic tests concerning the load capacity of the structure, its deflection as well as the technical and mycological condition of structural wooden elements.

2. MATERIALS AND METHODS

2.1. Description of the researched object

The Palace in Pawłowice (51°49′24,84″N 16°45′05,49″E, Fig. 1) is situated in the Greater Poland voivodeship, in the Leszno poviat, about 15 km east of Leszno. It was built at the end of the 18th century in the classicist baroque style based on Carl Gotthard Langhans' design. The Palace is erected on a rectangular plan, has three levels, and features two quarter-circle one-story arcaded galleries on both its sides. In 1923, as part of a major renovation, the staircase was moved from the vestibule to the rooms in the right wing, parquet floors were replaced, and electricity and central heating were installed.

Fig. 1. Location of the Palace and park complex in Pawłowice

The most representative room of the Palace is the great Column Hall (Fig. 2), which now serves as a conference room. Since 1945, the Palace has belonged to Zootechniczny Zakład Doświadczalny (Experimental Station), the branch of Instytut Zootechniki in Krakow (National Research Institute of Animal Production). Currently, the Palace is used as a conference and hotel centre, and it is protected by the conservator-restorer of monuments. Both the palace and the adjacent park have been listed in the register of monuments since 1952 and 1965, respectively. The manner of use of the building was extended, which brought in the necessity for performing strength calculations and for assessing the technical condition of the ceiling under the great Column Hall (Fig. 2). Social meetings held in this room increased the load acting on the ceiling, which showed deflections, cracks, and scratches. The occurrence of mycological and moisture damage to wooden elements carrying the main loads was also highly possible.

Fig. 2. Column Hall of the Palace in Pawłowice

2.2. TLS measurement

Terrestrial Laser Scanning is a technique that uses laser light for measurements. The measured object is illuminated by a beam which then, reflected from the object, returns to the scanner. Phase scanners, more commonly used today, can record up to approx. 1,000,000 measurement points per second. By knowing the distance (L) between the scanner and the i-th measurement point, vertical angle (β) and horizontal angle (α) coordinates of a point in a 3D coordinate system in real time can be calculated using the equation:

$$\begin{cases} X_i = L\cos\beta\cos\alpha, \\ Y_i = L\cos\beta\sin\alpha, \\ Z_i = L\sin\beta. \end{cases} \tag{1}$$

The on-site inspection consisted in carrying out an inventory of three rooms located directly under the Column Hall to estimate its geometry, in particular the deformation of the ceiling. The inventory was also aimed at indicating places for making test holes that enabled us to identify the location of ceiling beams. This significantly minimized the structural interference in the ceiling (the object is under conservation protection) of this historic building and allowed us to drill test holes in places that did not violate the structure of the ceiling. Scanning with the Faro Focus S70 laser scanner was conducted at 8 measuring stands in the rooms in question (Fig. 3). The manufacturer states that the accuracy of distance measurement is ± 1 mm, the 3D position accuracy on 25 m is 3.5 mm and the angular resolution is equal to 19 arcsec. The laser wavelength is 1550 nm, and the laser beam divergence is 0.3 mrad.

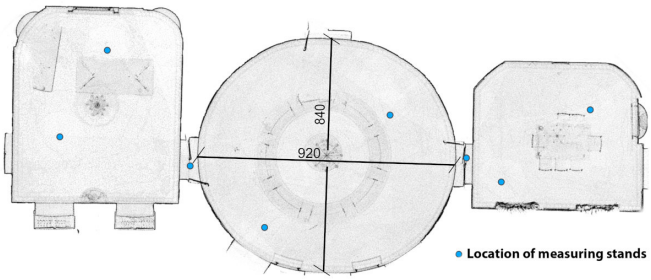

Fig. 3. Location of measuring stands

The average scanning time per 1 measuring stand was about 10 minutes, the scans were made with a resolution of 10240 × 4267 points. The distance between the measurement points on the measured plane was 6.1 mm/10 m with 4-times the quality. Properly prepared individual scans were combined in Faro Scene, creating a coherent point cloud consisting of approximately 157 million points. In the scanning process, reference spheres were used, which in later processing significantly facilitated the process of connecting clouds of points obtained from individual measuring stands.

The point cloud was then processed in CloudCompare to filter out the noise and perform an analysis of the ceiling geometry. First, CloudCompare arbitrarily generated a horizontal reference plane, which served as the basis for comparing the position of the point cloud of the analysed ceiling. Normal distances of individual points to the plane were determined, a cross-section was generated, and a profile of the ceiling face was developed according to the greatest changes in the geometry.

2.3. Dimensioning with the limit state method

There are two limit states: ultimate limit state and serviceability limit state. The design of wooden structures should be carried out in accordance with Eurocode 5 [38].

The ultimate limit state was calculated based on the following formulas, assuming bending along fibres. Thus, it was taken that the element was exposed to stresses only along one of the main axes:

$$k_m \frac{\sigma_{m,y,d}}{f_{m,y,d}} + \frac{\sigma_{m,z,d}}{f_{m,z,d}} \leq 1, \tag{2}$$

$$\frac{\sigma_{m,y,d}}{f_{m,y,d}} + k_m \frac{\sigma_{m,z,d}}{f_{m,z,d}} \leq 1, \tag{3}$$

where:

$\sigma_{m,y,d}$, $\sigma_{m,z,d}$, – design bending stresses, determined with regard to main axes of the cross-section,

$f_{m,y,d}$, $f_{m,z,d}$ – design bending strengths corresponding to bending stresses,

k_m – coefficient of redistribution of bending stresses in the cross-section (for a rectangular cross-section $k_m = 0.7$).

The load-bearing capacity of ceiling beams, assuming bending in one plane (bending in relation to the weaker axis of the cross section), was calculated according to the equation:

$$\sigma_{m,z,d} = \frac{M_{z,d}}{W_{y,n}} \leq k_{\text{crit}} f_{m,z,d}\,, \tag{4}$$

where:

$M_{z,d}$ – bending moment in the cross section,

$W_{y,n}$ – strength index about the y-axis, k_{crit} – buckling factor (for an element protected against buckling $k_{\text{crit}} = 1.0$).

The serviceability limit state was verified based on equations (5)–(8), assuming that the final deflection u_{fin} from a combination of different actions should be considered as the sum of separately defined deflections for each action:

$$u_{\text{fin}} = u_{\text{fin},G} + u_{\text{fin},Q_1} + u_{\text{fin},Q_i}\,, \tag{5}$$

where:

$$u_{\text{fin},G} = u_{\text{inst},G}(1 + k_{\text{def}}), \tag{6}$$

$$u_{\text{fin},Q_1} = u_{\text{inst},Q_1}(1 + \psi_{2,1} k_{\text{def}}), \tag{7}$$

$$u_{\text{fin},Q_i} = u_{\text{inst},Q_i}(1 + \psi_{2,i} k_{\text{def}}), \tag{8}$$

$u_{\text{fin},G}$ – final deflection from permanent action,

$u_{\text{inst},G}$ – temporary deflection from permanent action,

k_{def} – factor for deflection increase over time due to the combined effect of material creep and changes in moisture content,

$u_{\text{fin},Q1}$ – final deflection from variable action (first significant variable action),

$u_{\text{fin},Qi}$ – final deflection from variable action (successive variable action),

$u_{\text{inst},Q1}$ – temporary deflection from variable action (first significant variable action),

$u_{\text{inst},Qi}$ – temporary deflection from variable action (first significant variable action),

$\psi_{2,1}$ – coefficient for the combination value of variable action (first significant variable action),

$\psi_{2,i}$ – coefficient for the combination value of variable action (successive variable action).

Verification of the ultimate limit state requires the adoption of design values of actions, whereas for the serviceability limit state, the characteristic values are assumed. The design value of loads should be determined according to the equation:

$$X_d = k_{\text{mod}} \frac{X_k}{\gamma_M}\,, \tag{9}$$

where:

X_k – characteristic value for material strength, i.e. $f_{m,\,k}$,

γ_M – partial safety factor for material properties,

k_{mod} – modification factor for the duration of load and moisture content.

2.4. Methodology of moisture content and mycological tests

Mycological and moisture content tests of wooden elements were carried out using non-destructive (moisture content) and destructive (mycological) methods. Moisture content was measured using the qualitative method with capacitive moisture sensors and dielectric measurement, allowing for obtaining results without the need to sink the electrodes into the sampling material. When hard wood is analysed, the parameters of the TERMIO BM40 recorder are a significant advantage, the measurement range of which is between 0–50% and the resolution is 0.1% for wood and 0.1°C for temperature. The device can operate in a temperature-varied environment ranging from –5 to +50°C. Its optimal clamping force, when applied to the exposed web of the ceiling beam along fibres, is 10N. The measurement depth was 50 mm.

The mycological analysis was carried out in previously selected places, where subsequently test holes were made, with two methods of collecting pathogens [39, 40]. The non-invasive method was used to collect the sample by rubbing the selected places with sterile swabs, each time from an area of 100 cm^2. The destructive method, from each sample, under full aseptic conditions, consisted in splitting off a fragment of the ceiling beam with a decontaminated sterile swab. The beam was sampled in its 1/5 thickness. The presence of fungal structures in the provided samples obtained with the destructive method was assessed by dividing them into 100 one-millimetre fragments, which were laid out with 50 one-millimetre inoculate on PDA (glucose-potato agar). The colonies that grew were counted and identified by species. This method assumes that the share of fungal or bacterial colonies in more than 20% of material fragments laid out on the culture medium indicates a strong growth of microorganisms. The samples obtained with the non-destructive method were put into a flask containing 100 ml of 0.9% NaCl. After 5 minutes of shaking, 1 ml of suspension featuring propagating particles of microorganisms was taken from the vessel and applied to flasks with a known volume of 0.9% NaCl. After applying 1 ml of the mixture to solidified culture media (PDA and Sabouraud's medium), the objective was to obtain no more than 10–15 colonies on a Petri dish. The colonies that grew were counted and the known titre of the suspension, regardless of dilution, allowed for calculating the number of units forming microbial colonies (CFU) over 100 cm^2. The criteria for assessing the presence of propagating particles on the tested surfaces were adopted in accordance with HACCP recommendations (Hazardous Analytical Control Points), compliantly with Draft European Standard CEN/TC/243/WG2/1993.

The obtained colonies below the value of 20% are considered random. However, the criterion does not apply to domestic fungi. Here, even one colony indicates wood contamination.

The occurrence of surface and deep condensation was verified with the non-destructive method using the Trotec BP25 "dew point" temperature scanner. Diagnostics were carried out in test holes made from the room on the ground floor of the Palace, i.e. in the ceiling of the Column Hall. The scanner mea-

sures the temperature using an infrared light sensor. The measuring accuracy is ±3.5°C, for +20°C and air humidity ±3.5%. In total, three measurements were made in two test holes.

3. RESULTS

3.1. Measurements of the ceiling geometry

Measurements of the geometry of the ceiling and its inventory, in the rooms located directly under the Column Hall, were made with 3D laser scanning techniques (TLS). Scanning was carried out at eight measuring stands ensuring the continuity of point clouds (Fig. 3). The resultant point clouds were then combined into one point cloud in Faro Scene. The accuracy of connection of point clouds is at the level of Maximum Point Error 1.6 mm, Mean Point Error 1.2 mm, Minimum Overlap 56.2% with the maximum error in determining the distance Max. Distance Error 2.8 mm.

Initially, in Faro Scene, the point cloud was imported to CloudCompare. The cloud was processed to reduce noise and extract only the points that formed the ceiling geometry. Then a horizontal reference plane was introduced. Figure 4 visualizes the map of (normal) distances between the point cloud and the top-down adopted reference plane. As the arrangement of beams of the ceiling supporting structure was unknown, the position of the plane was assumed arbitrarily, and the developed distribution is a visualization of the map of the height of the ceiling face above the assumed comparative level (plane). Additionally, Fig. 5 shows the distribution of distances in the form of a histogram. The mean difference in the position of points (point cloud – reference plane) was 14 cm with a standard deviation of approx. 5 cm. The distribution of changes presented in Fig. 4 indicates that the ceiling is not horizontal, the differences also arose due to the method of finishing the ceiling – bas-relief (Fig. 6). Figure 4 also shows the profile of the ceiling face in cross-section with the greatest changes in its geometry between the entrances to side rooms. The difference between the highest point of the point cloud at the entrance to the room on the right side (Fig. 4 point 3) and the point at the entrance to the room on the left side (point 4) was as much as 12 cm. Similarly, the difference between point 1 and point 2 was 6.6 cm (measurements were made outside the outline of the existing stucco). It should be noted that the lime-cement plaster made on reed does not create a perfectly even surface, therefore, the measurement

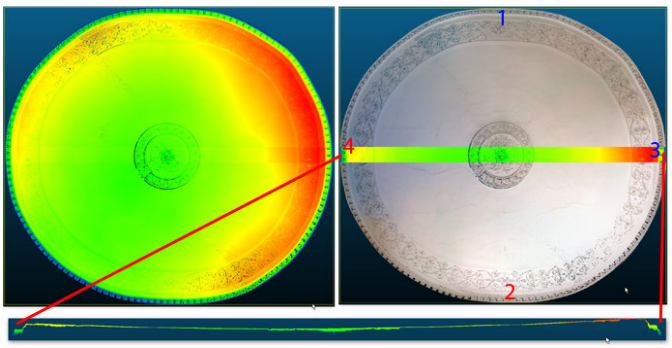

Fig. 4. Map of distances from the reference plane and profile of the geometry of the ceiling face

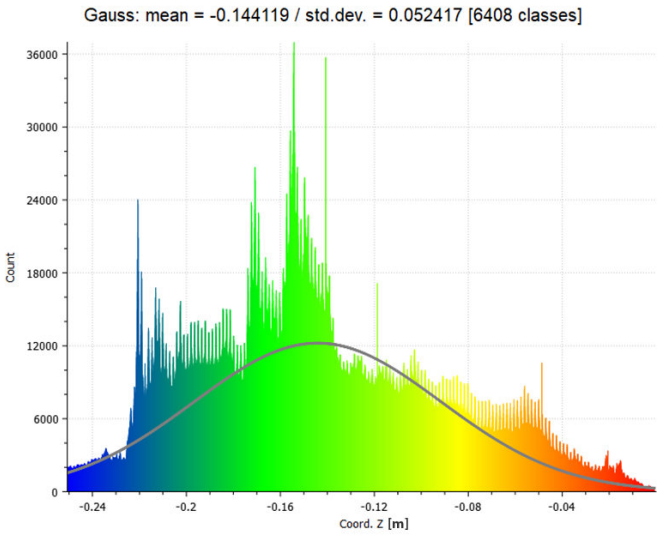

Fig. 5. Histogram of the distance of the ceiling face from the adopted reference plane for the entire point cloud

may be at risk of a large error and the location of ceiling beams alone cannot be concluded from it. Nowak et al. conducted similar studies of a historic building planned for reconstruction and adaptation [11], and, based on laser scanning, they estimated the ceiling deflection as 1.39 cm and the deviation of the front wall from the vertical plane by approx. 2 cm.

Fig. 6. Stucco on the ceiling (visible cracks in the plaster)

Only one series of measurements was made, therefore it was not possible to determine the deformation of the ceiling during its operation (when changing the ceiling load). It would require the imposition of additional load on the ceiling and re-inventory to obtain such data, for which the conservator's consent was not given.

However, the measurements carried out by means of laser scanning facilitated selecting the optimal location of places where endoscopic measurements were carried out and samples were taken for mycological tests.

3.2. Calculations of the load capacity and deflection of the ceiling

Based on the analysis of the ceiling geometry carried out using laser scanning, the places for test holes in the ceiling were selected. The part of the ceiling that was selected showed the greatest deflections during scanning. Before test holes were made, a reconnaissance opening had been drilled into which an

endoscopic inspection camera was inserted, allowing for identifying the location of ceiling beams. It significantly contributed to minimizing the interference in the ceiling structure in this historic building and helped select the location of test holes in the places that did not damage the ceiling structure (Fig. 7).

Fig. 7. View of the ceiling cross-section taken with an endoscopic camera

Two 10×15 cm test holes were made, the location of which is indicated on the projection (Fig. 8), whereas Fig. 9 shows the location of test holes in the room.

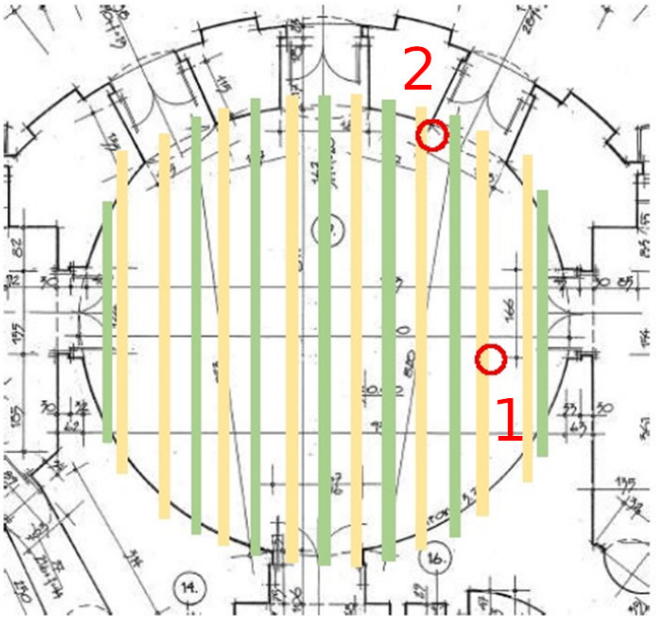

Legend: the beams of the lower system are marked in green; the beams of the upper system are marked in yellow; the locations of tesholes are marked in red, point 1 – the first test hole, point 2 – the second test hole.

Fig. 8. Partially recognized and plausible distribution of ceiling

Photos taken with an endoscopic camera and data from test holes allowed for making a drawing of the ceiling cross-section (Fig. 10) and a projection of the ceiling structure (Fig. 8).

Static calculations of the first and second limit states were made for the given ceiling structure of the Column Hall shown in Fig. 10. The purpose was to determine the maximum values

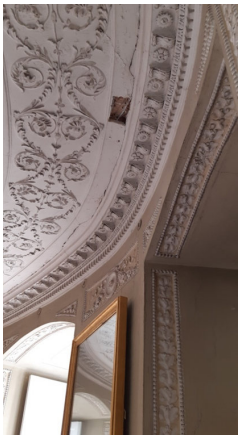

Fig. 9. Location of test holes

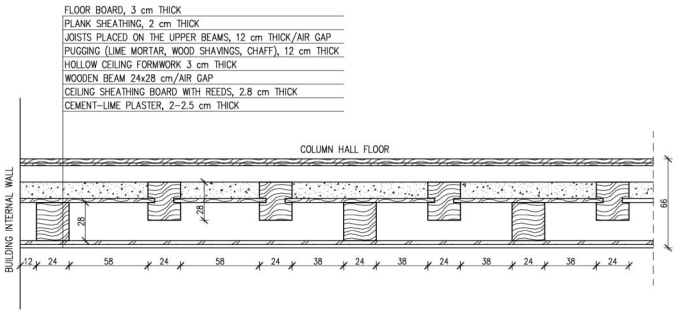

Fig. 10. Recognized cross-section of the ceiling

of service loads that the ceiling could carry. Therefore, the calculations of the ultimate limit state were made to estimate the highest possible value of service loads after considering permanent loads. For the serviceability limit state, the highest possible value of service loads was determined considering the maximum permissible deflection for ceiling beams.

The following assumptions were made for calculations:

- Use class 1 for a heated building (the class is characterized by a material moisture content corresponding to a temperature of 20°C and relative humidity of the ambient air exceeding 65% only for a few weeks a year. For class 1, the average moisture content of most types of coniferous wood does not exceed 12%).
- Wood class C35 with moisture content of 12–15% (the class was adopted due to the use of non-resinated wood for the ceiling, which significantly increases its strength). Strength properties of class C35: $f_{m,y,k} = 40$ MPa, $E_{0,\text{mean}} = 13$ GPa, $E_{0,05} = 8.7$ GPa.

The ceiling layers shown in Fig. 7 have loads with a characteristic value of 2.355 kN·m^{-2}. The span of the ceiling is 8.5 m. The following data is designated for ceiling beams with dimensions of 24×28 cm: $A = 672$ cm^2, $W_y = 3136$ cm^3, $I_y = 43904$ cm^4.

The bending strength about the y-axis is (y-axis is horizontal in the beam cross-section):

$$f_{m,y,d} = \frac{k_{\text{mod}} \cdot f_{m,y,k}}{\gamma_M} = \frac{0.7 \cdot 40}{1.3} = 21.54 \text{ MPa},$$

while the design load-bearing capacity of the wooden beam equals to:

$$M_{R,z,d} = W_y \cdot f_{m,z,d} = 67.55 \text{ kNm}.$$

Assuming the spacing between the central beams of 62 cm (Fig. 10) and for the static diagram of a single-span, free-supported beam, evenly loaded, the permissible service load was determined, which is 5.35 kN·m^{-2}. Consequently, the above calculation allows us to conclude that, based on the ultimate limit state calculation, it is possible to add (above the permanent load associated with ceiling layers) the ceiling/floor load in the Column Hall not exceeding 535 kg·m^{-2} (assuming a partial load factor $\gamma_F = 1.5$).

The serviceability limit state was verified using equations (5)–(8). Strength data of the wooden beams was adopted as in the analyses of the first limit state. The recommended deflection limit was taken based on [38] and it is $L_{ef}/250$ (where l_{ef} is the span of the beam). Eurocode 5 [38] facilitates, in the case of historic buildings, an increase in 50% of the deflection limit value. Thus, for the considered ceiling, the limit deflection is:

$$u_{\text{net,fin}} = \frac{L_{ef}}{250} \cdot 1.5 = 5.29 \text{ cm}.$$

The maximum service load, which can be added to the existing permanent load, was estimated by determining the deflection sagitta for a freely supported, uniformly loaded beam, for which the ratio is $l/h < 20$ (the length of the beam to its height). For permanent loads, the final deflection from permanent action $u_{\text{fin}, G}$ is:

$$u_{\text{fin},G} = \frac{5q_k L_{ef}^4}{384 E_{0,\text{mean}} I_y} = 3.16 \text{ cm}.$$

By subtracting the value of deflection from permanent loads from the limit deflection, the partial deflection of the beam can be determined, which can be used for service actions and amounts to $u_{\text{fin},G} = 2.13$ cm. By transforming equation (6), the value of service load $Q = 2.11$ kN·m^{-2} was calculated. Therefore, in addition to the permanent load, it is possible to add to the ceiling/floor in the Column Hall a load not exceeding 211 kg·m^{-2}.

3.3. Results of moisture content and mycological tests

The moisture content of selected ceiling elements (the representative places for analysing were selected based on the scanning method) is presented in Table 1. In total, in two test holes, 3 measurements were made.

Figure 11 shows exemplary moisture content measurement at measurement point no. 2.

Table 1

Results of moisture content measurement for three measuring points of wooden elements of the truss

Truss elements	Point no. 1	Point no. 2	Point no. 3
%	5.8	6.5	10.3

Fig. 11. Moisture content measurement of ceiling beams – test hole no. 2

Both standards: PN-EN 1995-1-1:2010 [38] and PN-B-03150-01:1981 [41] specify the permissible moisture content of coniferous wood, from which the analysed structural elements are made, depending on the conditions of their use, and according to the principle that their moisture content can be 2% lower or equal to usable moisture content. The permissible coniferous wood moisture content is 20% for structures protected against moisture and 23% for structures located in the open air.

According to the given criteria, the tested ceiling elements in the area near the external wall and in test holes, i.e. the most moisture-prone places, proved to be dry. In situ tests were carried out inside the Palace at maximum temperature $T = 16.9 - 17.7$°C and maximum moisture content 48–52%.

During the examination of the occurrence of condensation on the surface of the ceiling inside the rooms, no "dew point" was found. Also, no symptoms of wood decomposition were observed on the samples submitted for testing as well as no living structures, i.e. domestic fungi belonging to basidiomycetes (*Basidiomycota*) with strong wood decomposition capacity were found (Fig. 12).

Fig. 12. Petri dish after incubation (inoculation and the truncated tip from swabs for sample no. 1)

Figure 8 shows the representative places chosen for testing selected according to the results of scanning tests. The samples were taken compliantly with the following methodology. Sample no. 1 was collected non-destructively from the beam surface in test hole no. 1. Samples no. 2 and 3 were taken by the destructive method in test hole no. 1, whereas samples no. 4 and no. 5 were taken from test hole no. 2 by the destructive method. The test material was delivered in containers (Fig. 13).

Table 2 lists the species of fungi identified during examination.

Fig. 13. Exemplary sample of wood taken for laboratory tests

Table 2
Fungal species identified in samples

Species	Sample number				
	1	2	3	4	5
	Number of fungal colonies (CFU)				
Alternaria alternata	2	1	1		4
Asprgillus nidulans				1	
Cladosporium cladosporioides	3	3	12	5	3
Penicillium chrysogenum	8	4	4	8	6
Penicillium oxalicum		1			
Penicillium variabilae		2	2		1
Ulocladium botrytis	1			1	
Fungal colonies – total	14	11	19	15	14
Isolations %	14	11	19	15	14

Given mould fungi, it is assumed that the presence of fungal structures (CFU) in the tested material of up to 20% does not indicate the existence of favourable conditions for their growth. Such a level indicates natural contamination by fungal structures present in the immediate vicinity of the sampling site, i.e. in the air.

4. DISCUSSION

Most often we perceive historic objects as "sacrum", however, at present we are beginning to avoid this schematic thinking about our cultural heritage. The art of managing monuments and historic objects should consist of skilful balancing between the protection of original historic values and commercial and financial considerations. The authors in [42–44] referred to the diagnostics of historic buildings to use them as sacred, museum, hotel, educational or recreational facilities, providing the most advantageous methods of multidisciplinary and sustainable historic protection. They described technical and legal problems related to adaptation to modern requirements, i.e. safety of use, fire protection, and proper energy performance. The assessment of the load-bearing capacity of historic buildings is a completely different matter, in which modern load standards cannot be used, as most of these structures would not meet current requirements. The works [45–47] show the method of calculating the load-bearing capacity for historic buildings and explain the accepted deviations.

It is difficult to carry out diagnostic tests in historic buildings since they are usually under conservation protection and all methods, particularly the ones that consist of destructive diagnostics, are impossible to apply. Therefore, the laser scanning technique proposed in this study, performed as the first examination to determine the places for test holes, is an excellent solution as non-destructive, not interfering with the matter of the historic building. The use of laser scanning can significantly facilitate the assessment of damage and the proposition of an appropriate renovation system [11]. The accuracy of point clouds is sufficient to perform surface regularity checks. Boshe and Guenet [48] carried out relevant experiments by performing a surface flatness check using TLS. They also indicated that it is not necessary to conduct extremely dense scans, which consequently translates into saving time otherwise required for making measurements. The moisture analysis of historic buildings should be carried out thoroughly, the best results are obtained by conducting in situ examinations [49]. Mycological tests reveal the presence of various species of fungi, in particular toxicogenic and wood-degradable species. The methodology of mycological studies, on the basis of which the determination and counting of pathogen colonies are conducted, is well documented in the literature and has been used for years [39, 40, 50–52]. The samples did not show the presence of microorganisms considered pathogenic in amounts above average, as described in the Directive [53] of the European Parliament and the Council of Europe of September 18, 2000 as organisms of the 2nd and 3rd groups of danger, i.e. causing disease. Also, the presence of species posing a threat to health, listed in the Regulation of the Minister of Health of April 22, 2005 on harmful biological factors for health in the work environment and protection of the health of workers professionally exposed to these factors, was not found (Journal of Law, 2005 No. 81, item 716) [54].

5. CONCLUSIONS

"The future is a present made from the past". André Malraux's words make us consider and reflect on the importance of protecting historic buildings. The paper shows, on the example of a historic palace located in western Poland, the course of action and the results of diagnostics of one of the rooms in the facility for which a change in the manner of use was planned. Based on the tests and calculations performed, it can be concluded that:

Laser scanning is an efficient tool for the initial analysis of objects/buildings, i.e. it identifies the places with the greatest deflection or displacement for further invasive diagnostics.

The large deflections of the ceiling, which were revealed by laser scanning, were not confirmed by calculations. Therefore, it is concluded that they may be caused by structural imperfections created during construction. The flexibility of the floor may be due to poor stabilisation of the wooden floor constructed on joists. Undoubtedly, the structure of the ceiling is also important, primarily the layer of plaster applied on the reed, which

may be subject to large bending and, consequently, susceptible to scratches and cracks in every direction,

Based on the measured ceiling geometry, the places with the greatest deflections were selected for making test holes, which allowed us to recognize the ceiling structure and collecting wood samples for moisture content and mycological tests,

The performed calculations of wooden ceiling beams with the limit state method showed that in the case of the ultimate limit state, the additional service load that can be added is 535 kg·m^{-2}, while in the case of the serviceability limit state, the value of the additional maximum service load should not exceed 211 kg·m^{-2}.

After the calculations, it can be concluded that the serviceability limit state turned out to be decisive in terms of the possibility of using the Column Hall, because it will be exceeded when applying a load exceeding 2.11 kN·m^2,

The number of units forming the colonies of mould fungi in the collected samples was low. In the tested samples, no fungi were found that could pose a threat to structural elements in terms of biological corrosion,

The level of the presence of fungal structures does not indicate favourable conditions for their development,

Additionally, based on macroscopic examinations of the discovered fragments of the ceiling structure, it was found that there was no insect damage in the analysed places,

The samples did not show the presence in dangerous amounts of microorganisms considered pathogenic or expressed similarly.

The moisture tests of wood did not confirm any damage to the element, the level of moisture content was 5.8–10.3%, i.e. it did not exceed the value for structures protected against moisture, assuming class 1 use of the structure.

The air temperature distribution in the room ranged between 16.9 and 17.4°C for several days of the study. The tests showed that there is no possibility of surface and deep condensation within the tested ceiling.

Thanks to the proposed diagnostic methodology, large fragments of the historic ceiling were not damaged in this analysis. Based on examinations carried out in the selected test holes, the structural system of ceiling beams as well as their design and structure were identified. It was specified that it is a double ceiling, also known as "quiet". The identified cracks on the plaster surface do not show an alarmist state of the ceiling under the Column Hall, and the performed limit state calculations determine the values of the permissible service loads of the hall.

REFERENCES

[1] B. Nowogońska, "Consequences of Abandoning Renovation: Case Study – Neglected Industrial Heritage Building," *Sustainability*, vol. 12, no. 16, p. 6441, 2020.

[2] B. Nowogońska, "Intensity of damage in the aging process of buildings," *Arch. Civ. Eng.*, vol. 66, no. 2, 2020.

[3] B. Nowogońska and J. Korentz, "Value of technical wear and costs of restoring performance characteristics to residential buildings," *Buildings*, vol. 10, no. 1, p. 9, 2020.

[4] M. Lemmens, Ed., *Geo-information: Technologies, Applications and the Environment*. Dordrecht: Springer Netherlands, 2011.

[5] X. J. Cheng and W. Jin, "Study on reverse engineering of historical architecture based on 3D laser scanner," in *J. Phys. Conf. Ser.*, p. 160.

[6] J. Szolomicki, Ed., *Application of 3D laser scanning to computer model of historic buildings*, 2015.

[7] A. Skwirosz and K. Bojarowski, "The Inventory and Recording of Historic Buildings Using Laser Scanning and Spatial Systems," in *2018 Baltic Geodetic Congress (BGC Geomatics)*, pp. 340–343.

[8] P. Gleń and K. Krupa, "The use of 3D scanning for the inventory of historical buildings on the example of the palace in Snopków," *Teka Komisji Architektury, Urbanistyki i Studiów Krajobrazowych*, vol. 15, no. 2, pp. 73–78, 2019.

[9] T. Lipecki, "Geodetic and Architectural Inventory of the Historic Wooden Church of St. Szczepan in Mnichów (Poland) in Terms of Safety Assessment of the Geometric Condition of the Structure," 2020.

[10] N. Lercari, "Monitoring earthen archaeological heritage using multi-temporal terrestrial laser scanning and surface change detection," *J. Cult. Heritage*, vol. 39, pp. 152–165, 2019.

[11] R. Nowak, R. Orłowicz, and R. Rutkowski, "Use of TLS (LiDAR) for building diagnostics with the example of a historic building in Karlino," *Buildings*, vol. 10, no. 2, p. 24, 2020.

[12] W. Buczkowski, A. Szymczak-Graczyk, and Z. Walczak, "Experimental validation of numerical static calculations for a monolithic rectangular tank with walls of trapezoidal cross-section," *Bull. Pol. Acad. Sci. Tech. Sci.*, vol. 65, no. 6, pp. 799–804, 2017.

[13] M. Bernat, A. Janowski, S. Rzepa, A. Sobieraj, and J. Szulwic, "Studies on the use of terrestrial laser scanning in the maintenance of buildings belonging to the cultural heritage," *14th Geoconference on Informatics, Geoinformatics and Remote Sens.*, SGEM. ORG, Albena, Bulgaria, vol. 3, pp. 307–318, 2014.

[14] J. Liu, Q. Zhang, J. Wu, and Y. Zhao, "Dimensional accuracy and structural performance assessment of spatial structure components using 3D laser scanning," *Autom. Constr.*, vol. 96, pp. 324–336, 2018.

[15] J. Kwiatkowski, W. Anigacz, and D. Beben, "A case study on the noncontact inventory of the oldest european cast-iron bridge using terrestrial laser scanning and photogrammetric techniques," *Remote Sens.*, vol. 12, no. 17, p. 2745, 2020.

[16] A. Borkowski and G. Jóźków, "Accuracy assessment of building models created from laser scanning data," *International Archives of the Photogrammetry, Remote Sens., and Spatial Information Sciences*, vol. 39, B3, 2012.

[17] P. Klapa, B. Mitka, and M. Zygmunt, "Study into point cloud geometric rigidity and accuracy of TLS-based identification of geometric bodies," in *IOP Conf. Ser.: Earth Environ. Sci*, vol. 95, p. 32008, 2018.

[18] M. Zámečníková, A. Wieser, H. Woschitz, and C. Ressl, "Influence of surface reflectivity on reflectorless electronic distance measurement and terrestrial laser scanning," *J. Appl. Geod.*, vol. 8, no. 4, pp. 311–326, 2014.

[19] B. Schmitz, C. Holst, T. Medic, D. D. Lichti, and H. Kuhlmann, "How to efficiently determine the range precision of 3d terrestrial laser scanners," *Sensors*, vol. 19, no. 6, p. 1466, 2019.

[20] P. Gleń and K. Krupa, "Comparative analysis of the inventory process using manual measurements and laser scanning," *Budownictwo i Architektura*, vol. 18, no. 2, pp. 021–030, 2019.

[21] S. El-Omari and O. Moselhi, "Integrating 3D laser scanning and photogrammetry for progress measurement of construction work," *Autom. Constr.*, vol. 18, no. 1, pp. 1–9, 2008.

[22] G. Rocha, L. Mateus, J. Fernández, and V. Ferreira, "A scan-to-BIM methodology applied to heritage buildings," *Heritage*, vol. 3, no. 1, pp. 47–67, 2020.

[23] H. E.-D. Fawzy, "3D laser scanning and close-range photogrammetry for buildings documentation: A hybrid technique towards a better accuracy," *Alexandria Eng. J.*, vol. 58, no. 4, pp. 1191–1204, 2019.

[24] P. Grussenmeyer *et al.*, "Recording approach of heritage sites based on merging point clouds from high resolution photogrammetry and terrestrial laser scanning," *Int. Arch. Photogramm. Remote Sens. Spat. Inf. Sci*, vol. 39, pp. 553–558, 2012.

[25] F. Remondino, "Heritage recording and 3D modeling with photogrammetry and 3D scanning," *Remote Sens.*, vol. 3, no. 6, pp. 1104–1138, 2011.

[26] C. Sahin *et al.*, "Producing 3D city model with the combined photogrammetric and laser scanner data in the example of Taksim Cumhuriyet square," *Optics Lasers Eng.*, vol. 50, no. 12, pp. 1844–1853, 2012.

[27] C. Biagini, P. Capone, V. Donato, and N. Facchini, "Towards the BIM implementation for historical building restoration sites," *Autom. Constr.*, vol. 71, pp. 74–86, 2016.

[28] L. Mahdjoubi, C. Moobela, and R. Laing, "Providing real-estate services through the integration of 3D laser scanning and building information modelling," *Comput. Ind.*, vol. 64, no. 9, pp. 1272–1281, 2013.

[29] A. Osello, G. Lucibello, and F. Morgagni, "HBIM and virtual tools: A new chance to preserve architectural heritage," *Buildings*, vol. 8, no. 1, p. 12, 2018.

[30] F.J. López, P.M. Lerones, J. Llamas, J. Gómez-García-Bermejo, and E. Zalama, "A review of heritage building information modeling (H-BIM)," *Multimodal Technologies and Interaction*, vol. 2, no. 2, p. 21, 2018.

[31] S. Bruno, M. de Fino, and F. Fatiguso, "Historic Building Information Modelling: performance assessment for diagnosis-aided information modelling and management," *Autom. Constr.*, vol. 86, pp. 256–276, 2018.

[32] M. Andriasyan, J. Moyano, J. E. Nieto-Julián, and D. Antón, "From point cloud data to building information modelling: An automatic parametric workflow for heritage," *Remote Sens.*, vol. 12, no. 7, p. 1094, 2020.

[33] N. Kip and J. A. van Veen, "The dual role of microbes in corrosion," *The ISME J.*, vol. 9, no. 3, pp. 542–551, 2015.

[34] J. Singh, "Nature and extent of deterioration in buildings due to fungi 3," *Building Mycology*, p. 30, 1994.

[35] J. D. Miller, "Fungi as contaminants in *Indoor Air*," *Atmos. Environ.,. Part A. General Topics*, vol. 26, no. 12, pp. 2163–2172, 1992.

[36] K. Sterflinger, "Fungi: their role in deterioration of cultural heritage," *Fungal Biol., reviews*, vol. 24, 1-2, pp. 47–55, 2010.

[37] A. Szymczak-Graczyk, I. Laks, B. Ksit, and M. Ratajczak, "Analysis of the Impact of Omitted Accidental Actions and the Method of Land Use on the Number of Construction Disasters (a Case Study of Poland)," *Sustainability*, vol. 13, no. 2, p. 618, 2021.

[38] *Eurokod 5 – Projektowanie konstrukcji drewnianych – Część 1-1: Postanowienia ogólne – Reguły ogólne i reguły dotyczące budynków*, PN-EN 1995-1-1:2010 Eurokod 5, PN-EN 1995-1-1:2010 Eurokod 5.

[39] G.L. Barron, *The genera of Hyphomycetes from soil*. University of Glasgow (United Kingdom), 1984.

[40] M.B. Ellis, "Dematiaceous hyphomycetes: 1," *Mycological papers*, vol. 76, 1960.

[41] *Konstrukcje z drewna i materiałów drewnopochodnych – Obliczenia statyczne i projektowanie – Materiały*, PN-B-03150-01:1981, PN-B-03150-01:1981.

[42] E. T. Delegou, G. Mourgi, E. Tsilimantou, C. Ioannidis, and A. Moropoulou, "A multidisciplinary approach for historic buildings diagnosis: the case study of the Kaisariani monastery," *Heritage*, vol. 2, no. 2, pp. 1211–1232, 2019.

[43] F. Ascione, F. Ceroni, R. F. de Masi, F. de'Rossi, and M. R. Pecce, "Historical buildings: Multidisciplinary approach to structural/energy diagnosis and performance assessment," *Appl. Energy*, vol. 185, pp. 1517–1528, 2017.

[44] S. Fais, G. Casula, F. Cuccuru, P. Ligas, and M. G. Bianchi, "An innovative methodology for the non-destructive diagnosis of architectural elements of ancient historical buildings," *Sci. Rep.*, vol. 8, no. 1, pp. 1–11, 2018.

[45] P. B. Lourenço, "Computations on historic masonry structures," *Prog. Struct. Eng. Mater.*, vol. 4, no. 3, pp. 301–319, 2002.

[46] A. Iringová and R. Idunk, "Solution of fire protection in historic buildings," *Civ. Environ. Eng.*, vol. 12, no. 2, pp. 84–93, 2016.

[47] M. Gołdyn and T. Urban, "Failures of the Cast-Iron Columns of Historic Buildings—Case Studies," *Infrastructures*, vol. 5, no. 9, p. 71, 2020.

[48] F. Bosché and E. Guenet, "Automating surface flatness control using terrestrial laser scanning and building information models," *Autom. Constr.*, vol. 44, pp. 212–226, 2014.

[49] B. Ksit and M. Gaczek, "Analytical meanders of selected systems for thermo-renovation of historical buildings," in *E3S Web of Conferences*, vol. 49, p. 00062, 2018.

[50] G.A. de Vries, "Contribution to the knowledge of the genus Cladosporium Link ex Fr," *Contribution to the knowledge of the genus Cladosporium Link ex Fr*, 1952.

[51] K.B. Raper and D. I. Fennell, "The genus Aspergillus," *The genus Aspergillus*, 1965.

[52] K.B. Raper and C. Thom, "A manual of the Penicillia," *A manual of the Penicillia*, 1949.

[53] *Directive 2000/54/EC of the European Parliament and of the Councilof18 September 2000 on the protection of workers from risks r elated to exposure to biological agents at work. Official Journal of the European Communities*, 17.10.2000, Directive 2000/54/EC, L 262/21-45, Directive 2000/54/EC.

[54] *Rozporządzeniu Ministra Zdrowia z dnia 22 kwietnia 2005 w sprawie szkodliwych czynników biologicznych dla zdrowia w środowisku pracy oraz ochrony zdrowia pracowników zawodowo narażonych na te czynniki*, Dz. U z 2005 r. Nr 81, poz. 716, Dz. U z 2005 r. Nr 81, poz. 716.